GA–A25835

MOMENTUM CONFINEMENT AT LOW TORQUE

by
W.M. SOLOMON, K.H. BURRELL, J.S. deGrassie, R. BUDNY, R.J. GROEBNER,
W.W. HEIDBRINK, J.E. KINSEY, G.J. KRAMER, M.A. MAKOWSKI, D. MIKKELSEN,
R. NAZIKIAN, C.C. PETTY, P.A. POLITZER, S.D. SCOTT, M.A. VAN ZEELAND,
and M.C. ZARNSTORFF

JULY 2007

GENERAL ATOMICS

DISCLAIMER

GA–A25835

MOMENTUM CONFINEMENT AT LOW TORQUE

by
W.M. SOLOMON,* K.H. BURRELL, J.S. deGrassie, R. BUDNY,* R.J. GROEBNER,
W.W. HEIDBRINK,† J.E. KINSEY, G.J. KRAMER,* M.A. MAKOWSKI,‡
D. MIKKELSEN,* R. NAZIKIAN,* C.C. PETTY, P.A. POLITZER, S.D. SCOTT,*
M.A. VAN ZEELAND, and M.C. ZARNSTORFF*

This is a preprint of an invited paper presented at the 34th EPS Conf. on Plasma Physics, in Warsaw, Poland, July 2-7, 2007 and to be published in the *Proceedings.*

*Princeton Plasma Physics Laboratory, Princeton, New Jersey.
†University of California-Irvine, Irvine, California.
‡ Lawrence Livermore National Laboratory, Livermore, California.

Work supported by
the U.S. Department of Energy
under DE-AC02-76CH03073, DE-FC02-04ER54698,
SC-G903402, and W-7405-ENG-48

GENERAL ATOMICS PROJECT 30200
JULY 2007

GENERAL ATOMICS

Momentum Confinement at Low Torque

W. M. Solomon[1], K. H. Burrell[2], J. S. deGrassie[2], R. Budny[1], R. J. Groebner[2], J. E. Kinsey[2], G. J. Kramer[1], M. A. Makowski[3], D. Mikkelsen[1], R. Nazikian[1], C. C. Petty[2], P. A. Politzer[2], S. D. Scott[1], M. A. Van Zeeland[2], M. C. Zarnstorff[1]

[1] Princeton Plasma Physics Laboratory, Princeton University, Princeton, NJ 08543

[2] General Atomics, P.O. Box 85608, San Diego, California 92186-5608

[3] Lawrence Livermore National Laboratory, Livermore, California 94550

E-mail: wsolomon@pppl.gov

Abstract. Momentum confinement was investigated on DIII-D as a function of applied neutral beam torque at constant normalized beta β_N, by varying the mix of co (parallel to the plasma current) and counter neutral beams. Under balanced neutral beam injection (i.e. zero total torque to the plasma), the plasma maintains a significant rotation in the co-direction. This "intrinsic" rotation can be modeled as being due to an offset in the applied torque (i.e. an "anomalous torque"). This anomalous torque appears to have a magnitude comparable to one co-neutral beam source. The presence of such an anomalous torque source must be taken into account to obtain meaningful quantities describing momentum transport, such as the global momentum confinement time and local diffusivities.

Studies of the mechanical angular momentum in ELMing H-mode plasmas with elevated $q_{\min}$ show that the momentum confinement time improves as the torque is reduced. In hybrid plasmas, the opposite effect is observed, namely that momentum confinement improves at high torque/rotation. GLF23 modeling suggests that the role of $E \times B$ shearing is quite different between the two plasmas, which may help to explain the different dependence of the momentum confinement on torque.

PACS numbers: 52.25.Fi, 52.55.Fa

1. Introduction

Plasma rotation is widely acknowledged as playing an important and beneficial role in fusion plasmas. Examples include the improvement of confinement by the suppression of turbulence through $E \times B$ shear [1], and the ability to access higher performance plasmas through stabilization of plasma instabilities such as resistive wall modes [2]. Hence, the ability to predict rotation is highly desirable for estimating plasma performance in future devices. Understanding momentum transport, along with all sources and sinks of momentum in the plasma, is a necessary step in obtaining the predictive knowledge of rotation that we seek. In this sense, one of the difficulties in conducting careful studies in momentum transport is finding suitable target plasmas where one can have some confidence in the ability to treat the sources and sinks. For example, plasmas that are unstable to Alfvén eigenmodes [3, 4] may significantly alter the source profile from the classical computation. Other magnetohydrodynamic (MHD) instabilities coupled with error fields in the plasma may result in braking of the plasma rotation [5, 6], acting as an unaccounted for sink.

The recent reversal of one of the neutral beam lines on DIII-D has opened new possibilities for momentum transport studies. In particular, the new arrangement permits the decoupling of the neutral beam power and torque input, allowing studies to be made at low torque/rotation but still significant normalized beta, $\beta_N = \beta/(I_p/aB_\phi)$, where β is the volume-average percentage ratio of the plasma pressure to the magnetic pressure, I_p is the plasma current (in MA), a is the minor radius (in m), and B_ϕ the toroidal magnetic field (in T).

Investigations made at low net neutral beam torque reveal several key points. First, under conditions of zero net neutral beam torque, there persists a significant rotation in the direction of the plasma current (co-rotation). This rotation is related to the "intrinsic rotation" [7, 8, 9, 10] observed in the absence of auxiliary momentum input, although it is more complicated due to the details of the individual neutral beam torque profiles. It was determined that one additional counter neutral beam source was required to reduce the angular momentum in the plasma to zero. This indicates an anomalous torque source in the plasma, with a magnitude roughly equivalent to one neutral beam. The proper treatment of this intrinsic rotation (or anomalous torque) is critical in order to obtain meaningful values for quantities such as angular momentum confinement or momentum diffusivity.

The paper is organized as follows. First, a look at the dependence of momentum transport on applied torque is considered by investigating the global momentum confinement time in section 2. In particular, H-mode plasmas with edge localized modes (ELMs) and hybrid discharges are studied. In section 3, the local diffusivities are analyzed. Finally, the potential systematic bias in the analysis of momentum transport caused by anomalous fast ion transport due to MHD activity is investigated in section 4. A summary of the results is given in section 5.

2. Global momentum confinement time

2.1. ELMing H-mode plasmas with elevated $q_{\min}$

Momentum confinement was studied in ELMing H-mode plasmas, with minimum safety factor $q_{\min}$ elevated above one until approximately 5 s into the discharge such that $q_{\min} \sim 1.4$ during the times of interest presented in this paper. With $q_{\min} > 1$, the additional complication of the impact of sawteeth on rotation can be avoided. Various torque scans were performed at constant β_N, using the β-feedback control capability of the plasma control system to give matched energy conditions as the amount of counter neutral beam injection was changed. In these discharges, various levels of counter neutral beam power were added at 3 s, with the β-feedback adjusting the amount of co-beam injection to maintain the requested β_N level. Density and temperature profiles before and after the beam change are relatively similar. Rotation profile measurements of impurity carbon ions from charge exchange recombination spectroscopy (CER) [11, 12, 13] have been corrected for atomic physics distortions to the measured charge exchange spectrum [14, 15, 16, 17]. This is particularly important at low rotation and high temperatures, where the atomic physics effects are comparable to or greater than the true velocity.

Figure 1(a) shows the central toroidal velocity as a function of total integrated torque. Here, the total torque is obtained from TRANSP analysis [18], including effects of prompt loss. The data presented is averaged over approximately 300 ms of relatively steady state plasma conditions and several β_N scans are compiled together. No systematic dependence on the β_N level is indicated. The overall trend appears relatively linear at low torque values, although there does appear to be some flattening at large torque values, particularly in the core. Of particular interest is the region around zero total torque. As is shown in figure 1(a), there is a substantial central toroidal rotation near zero net neutral beam torque, exceeding 100 km/s in the center. This rotation at zero net torque is conceptually the same as the intrinsic rotation observed on many devices with no auxiliary torque input, although there is a subtle difference. Due to the different deposition profiles of the co and counter neutral beams, it will generally be the case that a plasma with zero total torque may have regions of significant positive and negative torque. Perhaps more surprising then is the fact that the rotation profile remains peaked and in the co-I_p direction even when the torque deposition profile is essentially zero out to $\rho \sim 0.7$ and counter outside of that. This reinforces the existence of an intrinsic rotation in these discharges (or perhaps more accurately, an anomalous source of torque, which will be described later). From the torque scan data, it is simple to interpolate the rotation profile to zero net torque, which is shown in Figure 1(b). Note that although this profile comes from impurity carbon measurements, the neoclassical corrections for the main ion deuterium tend to increase the amount of co-rotation.

The existence of the intrinsic rotation can be seen even more clearly when considering the total mechanical angular momentum as a function of applied neutral beam torque, as shown in figure 2. As before, the data is obtained by averaging over a 300 ms time window. We see again that at zero net neutral beam torque, there is significant angular momentum in the co-direction. It is also clear that there is a non-linear response of the angular momentum to the applied torque. A hint of this type of behavior can be seen in data from PBX-M [19].

The global momentum confinement time, τ_ϕ, represents the decay of angular momentum, L from the plasma. A simplified model for the evolution of the angular momentum can be written as

$$\frac{dL}{dt} = T - \frac{L}{\tau_\phi}, \tag{1}$$

where T is the source of momentum, typically the torque from the neutral beams. Under steady state conditions when the angular momentum is not evolving, the left hand side is zero, and the momentum confinement time is simply given by $\tau_\phi = L/T$. It is apparent that using this expression for the momentum confinement time will cause $\tau_\phi \to \infty$ if the torque goes to zero while the angular momentum remains finite, as is the case here. Clearly the proper treatment of the intrinsic rotation is crucial in order to make meaningful assessments of momentum transport.

If we consider the intrinsic rotation as a constant offset that the neutral beam driven rotation builds upon, then we can get an estimate of the beam driven momentum confinement time by subtracting this offset from all the data, $\tau'_\phi = (L - L_0)/T$, effectively giving us an "incremental" momentum confinement time. Note that this effectively slides the curve in figure 2 down so as to cross the origin. The non-linear response of the angular momentum to the torque can be modeled very well by a simple quadratic function, $L - L_0 = aT - bT^2$, where a and b are positive constants, as illustrated by the overlaid dashed curve in figure 2. Such a response of the angular momentum immediately implies a linear degradation of momentum confinement with neutral beam torque, since $\tau'_\phi = (L - L_0)/T = a - bT$.

A better approach than simply subtracting the intrinsic rotation is to actually account for the anomalous torque that causes it, so as to recover an estimate of the true momentum confinement time. With the present data set, we can actually infer the anomalous torque profile directly.

Figure 3 shows the toroidal rotation frequency profile during a phase where there are three neutral beam sources: one co ($\sim$ 2.5 MW) plus two counter ($\sim$ 5 MW). Despite the fact that there is one net counter source being applied, the rotation is basically zero across the entire plasma profile. This rotation profile is constant for several hundred milliseconds while these beams are being applied.

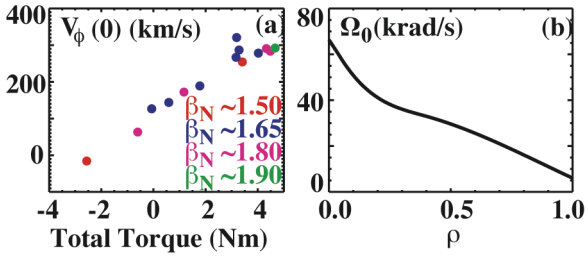

Fig. 1. (a) Central toroidal velocity vs total integrated torque. (b) Estimated intrinsic rotation profile, obtained from torque scan by interpolating the measured rotation profiles to zero total integrated torque.

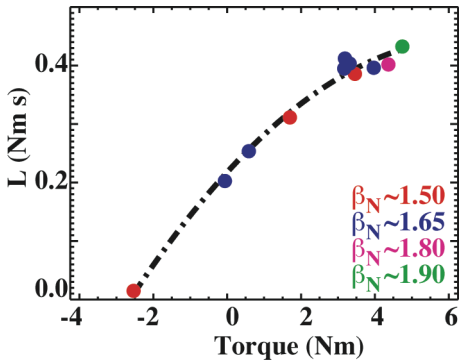

Fig. 2. Total mechanical angular momentum in the plasma as a function of applied neutral beam torque. The angular momentum data exhibits a nonlinear response to torque.

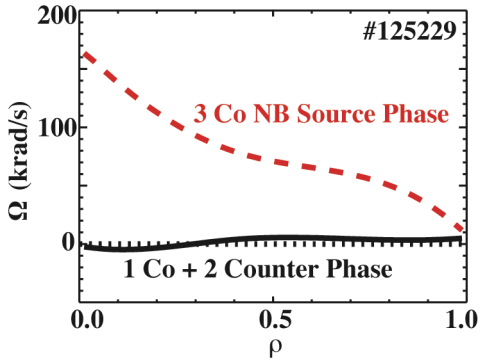

Fig. 3. Rotation frequency profiles with one co + two counter neutral beam sources. With one net counter source applied, the rotation is effectively zero across the profile. For reference, the 3 co NB source phase is also shown.

From the momentum balance equation, the toroidal velocity, V_ϕ evolves according to $mnR\partial V_\phi/\partial t = \eta + \nabla \cdot \Gamma_\phi$, where η is the local torque density,

$$\Gamma_\phi = mnR\left(\chi_\phi \frac{\partial V_\phi}{\partial r} + V_\phi V_\phi^{\text{pinch}}\right) \tag{2}$$

is the toroidal momentum flux, χ_ϕ is the local momentum diffusivity and V_ϕ^{pinch} represents a convective pinch velocity of momentum.

In the case where the rotation profile is zero everywhere across the profile and not evolving, then it is clear that there cannot be any net source of momentum into the plasma, since all the other terms (i.e. V_ϕ, $\partial V_\phi/\partial r$, $\partial V_\phi/\partial t$) are zero. This situation is almost ideally realized here, and so apparently we have an anomalous source of torque balancing out the residual from the 2 counter + 1 co source. Hence, to a first approximation, our anomalous torque profile must be the negative of the net computed neutral beam torque profile, so as to cancel it out. Accordingly, the anomalous torque source must integrate to approximately one co source. Essentially, the plasma is rotating as if there were an additional co neutral beam source being injected into the plasma.

One can of course imagine other off diagonal terms for the momentum flux equation 2, but as a matter of practicality, any terms that are not proportional either to velocity or the gradient of the velocity are effectively equivalent to a torque source.

We can actually refine our estimate of the anomalous torque profile by making use of the torque scan data. At each radius, the integrated angular momentum to that radius can be plotted against the integrated neutral beam torque to that radius. At all radii, the data shows a fairly linear dependence over this restricted range. For this sequence of plots, we can therefore find the x-intercept at each radius, corresponding to the amount of neutral beam torque required to offset the intrinsic rotation and bring the angular momentum to zero. The anomalous torque will be the negative of this quantity.

In this manner, we can determine the integrated anomalous torque profile, shown in figure 4(a). Overplotted is the negative of the integrated torque profile corresponding to the conditions in figure 3. Hence, this interpolation technique provides a refinement compared to the actual data obtained. In figure 4 (b), the torque density profile is backed out. The torque is largely concentrated towards the edge of the plasma, although there appears to be some significant torque in the core also.

Although it is not clear what is generating this extra torque, several recent theories point to effective torque sources near the edge, resulting from gradients in quantities other than V_ϕ giving off-diagonal terms in the neoclassical theory (e.g. Ref. [20]), or generated by turbulence through the Reynolds stress [21]). Additional experiments would be required to figure out whether the data here is consistent with such theories. Another possibility is that the calculated fast ion profile is simply incorrect, for example, due to Alfvénic activity. This will be discussed further in section 4.

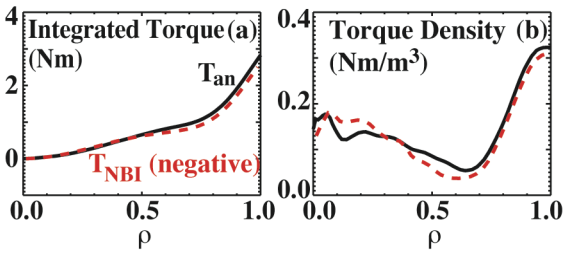

Fig. 4. (a) Anomalous torque profile as approximated by the negative of the neutral beam torque when V_ϕ is close to zero across the whole profile (green - - - -) and as interpolated from the torque scan (red). Including the effects of anomalous fast ion transport to match the measured neutron rate and stored energy modifies the inferred anomalous torque profile (blue). (b) Inverted anomalous torque density profile.

Now that we have determined this additional source of torque in the plasma, $T_{\rm an}$, we can go back and compute the global angular momentum time, including this source, $\tau_\phi^* = L/(T_{\rm NBI} + T_{\rm an})$. This corrected momentum confinement time is shown in figure 5. Not surprisingly, we still recover a momentum confinement time exhibiting a linear degradation of momentum confinement with increased torque. In some sense, this degradation of momentum confinement with increased torque is somewhat analogous to the more familiar degradation of energy confinement with increased power. Note that because of the relatively large anomalous torque, the values on the total torque axis have shifted significantly, and the scan never actually makes it to the counter torque side, which is of course consistent with the fact that the the angular momentum was always positive in these scans.

As with the analysis of the incremental momentum confinement time, this approach still requires that we assume that the intrinsic rotation or anomalous torque remains constant as we scan the torque. There are two separate considerations here. The first is that experiments to date have shown that there is a β_N scaling to the intrinsic rotation level [22]. In terms of the flattening of the angular momentum response at large torque, one can note that the data point closest to zero torque (from which we predominantly infer the anomalous torque) was obtained at $\beta_N \sim 1.65$. The two torque points at the highest torque in figure 2 correspond to those with $\beta_N > 1.65$, hence based on the usual scaling for intrinsic rotation, if anything, one might expect the intrinsic rotation to be even larger. This would make the curve get steeper, rather than flatten out, and hence does not appear to explain this result. The other possibility is that the intrinsic rotation level is reduced as more neutral beam torque is added. This would give the flattening of the angular momentum response that we observe. While that technically may be the case, from a practical point of view, there is no real difference between a reduction in the intrinsic rotation and a reduction in the momentum confinement time (although clearly the physics behind these two scenarios could be different).

As a cross-check to this result, we can also look at the dynamic behavior of the rotation as a torque perturbation is applied, in this case in the form of a step from one value to another. Such an analysis gives us the angular momentum relaxation time, which one might expect should be related to the global momentum confinement time. Referring to equation 1, the relaxation time can be obtained by integrating the model and solving for τ_ϕ. The angular momentum relaxation time $\tau_\phi^{\rm relax}$ obtained in this fashion exhibits the same degradation of momentum confinement with increasing torque as was determined for the steady state analysis, and is overplotted for reference in figure 5.

2.2. Hybrid plasmas

Detailed studies of the effect of rotation on confinement were also conducted in hybrid plasmas [23]. TRANSP analysis has similarly been performed on these discharges, and the resultant angular momentum response plot is shown in figure 6(a) for plasmas with $q_{95} \sim 4.5$, $q_{\rm min} \gtrsim 1$ and $\beta_N \sim 2.5$. It is clear that once again, there is a significant

amount of co-rotation at zero neutral beam torque, indicating a comparable level of intrinsic rotation as in the earlier ELMing H-mode plasmas. More striking, however, is the fact that the curvature of the angular momentum response is opposite to that of the previous case, that is, the change in angular momentum gets larger as the torque is increased. This suggests that the momentum confinement time actually improves with increased torque. Clearly, due to the intrinsic rotation, we again cannot simply divide the angular momentum by the torque for these steady state plasmas. Nonetheless, we can still construct the incremental momentum confinement time, τ'_ϕ, which is shown in figure 6(b). Note that we cannot deduce the anomalous torque for this dataset, because reducing the torque further caused the $m/n = 3/2$ neoclassical tearing mode to slow down and lock. The trend of the momentum confinement time versus torque is consistent with the expectation based on the response of the angular momentum to the torque.

GLF23 [24, 25] modeling has been undertaken to try to understand the different responses to torque between the hybrid and ELMing H-mode plasmas. These simulations take the measured density, toroidal rotation and current profiles and then calculate the temperature profiles based on the gyro-Landau-fluid GLF23 transport model. Figure 7 summarizes these results. With $E \times B$ shearing turned on, GLF23 makes a reasonable prediction for the temperature profiles at high torque/rotation in the hybrid plasmas, but if the $E \times B$ shear is turned off, as in the dashed curve, then the agreement is considerably worse. At low rotation, not surprisingly, the GLF23 prediction of the temperatures is acceptable with or without $E \times B$ shearing, indicating that $E \times B$ shear is playing a lesser role in the confinement. In other words, the benefit of $E \times B$ shear on the turbulence is reduced along with the torque during these scans.

In contrast, GLF23 runs done for the ELMing H-mode plasmas with elevated $q_{\min}$ described in section 2.1 indicate a much weaker role of $E \times B$ shear even at large rotation. Hence, the trend observed in the elevated $q_{\min}$ plasmas may be speculated as an underlying effect, which is obscured in the case of the hybrids by the overwhelming change in $E \times B$ shear as the rotation is reduced. Future studies will investigate GLF23 predictions of the evolution of the toroidal rotation itself based on the torque input profiles from TRANSP.

As an aside, note that in figure 6(b) there is clearly more scatter in the data points than in the ELMing H-mode data, but more problematic, one point has come up with a negative momentum confinement time. In general, the 3/2 mode amplitude tended to increase with decreasing rotation [23], although there was considerable variation, which may contribute to increased scatter in the momentum confinement times.

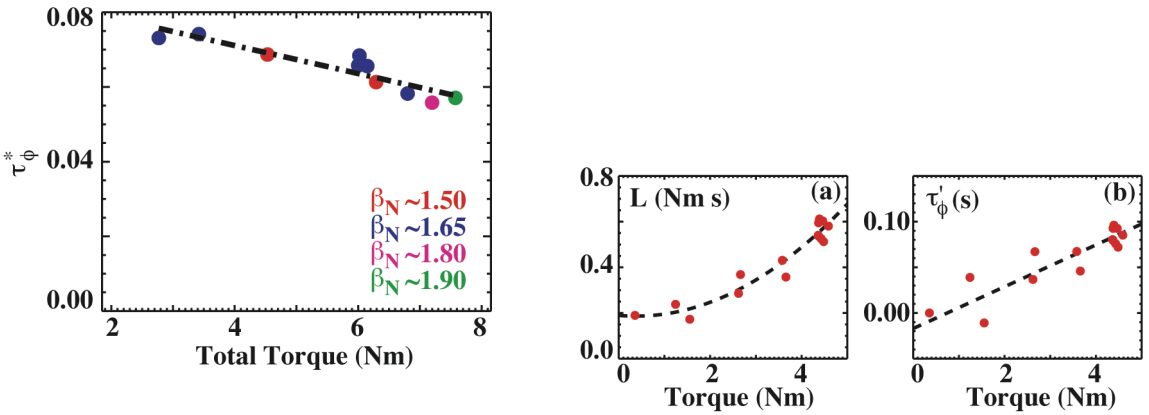
0.08
0.04
0.00
τ^*_ϕ
2
4
6
8
Total Torque (Nm)
β_N~1.50
β_N~1.65
β_N~1.80
β_N~1.90
0.8
0.4
0.0
L (Nm s)
(a)
0
2
4
Torque (Nm)
0.10
0.00
τ'_ϕ (s)
(b)
0
2
4
Torque (Nm)

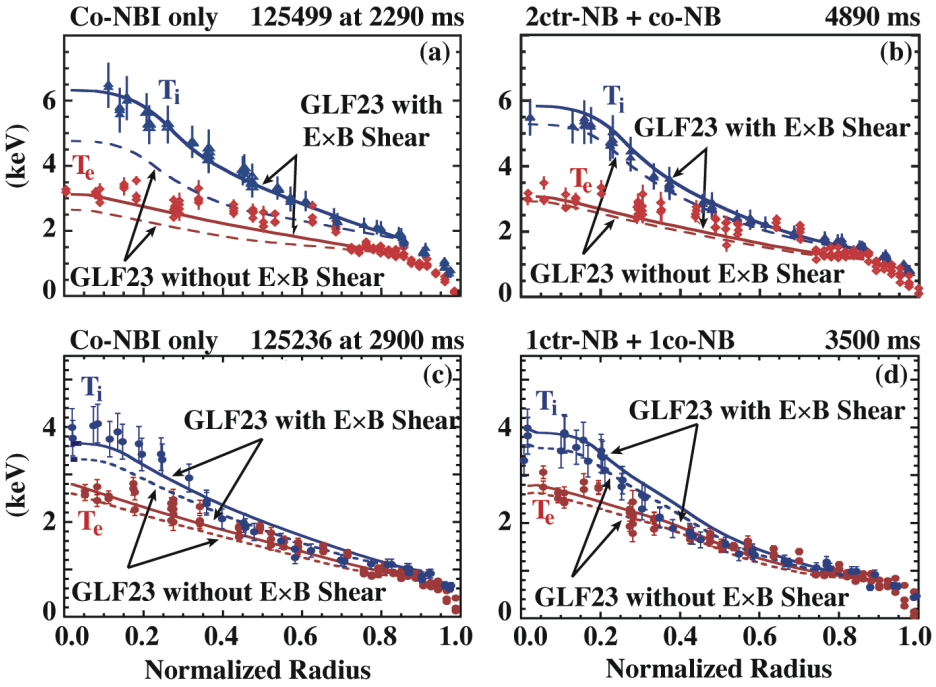
Co-NBI only 125499 at 2290 ms
(a)
T_i
GLF23 with E×B Shear
T_e
GLF23 without E×B Shear
(keV)
2ctr-NB + co-NB 4890 ms
(b)
T_i
GLF23 with E×B Shear
T_e
GLF23 without E×B Shear
Co-NBI only 125236 at 2900 ms
(c)
T_i
GLF23 with E×B Shear
T_e
GLF23 without E×B Shear
(keV)
1ctr-NB + 1co-NB 3500 ms
(d)
T_i
GLF23 with E×B Shear
T_e
GLF23 without E×B Shear
0.0
0.2
0.4
0.6
0.8
1.0
Normalized Radius
Normalized Radius

3. Local momentum and heat diffusivities

The local momentum diffusivities are solved as per equation 2, neglecting the convective pinch term, which cannot be readily separated in steady state analysis. If the momentum sources are not all being included in the momentum balance, then the fluxes will obviously not be computed correctly. If we have an additional anomalous source as identified earlier, then the momentum diffusivity needs to be corrected, $\chi_\phi^* = (1 + T_{\rm an}/T)\chi_\phi$. Figure 8 shows the momentum diffusivity for the ELMing H-mode plasmas described as a function of the local toroidal rotation at several radii across the plasma, corrected for the anomalous torque. Also shown is the ion heat diffusivity. There are a number of interesting observations. Firstly, the local momentum diffusivity increases with the local toroidal rotation outside of about mid-radius, and is roughly independent inside of that. This increase in momentum diffusivity is consistent with the degradation of momentum confinement with torque. Secondly, we see that at moderate to large toroidal rotations above 100 km/s, the momentum and heat diffusivities are comparable, at least inside of $\rho \sim 0.5$. However, we see that they begin to diverge significantly at low rotation values. Furthermore, the heat diffusivity shows some hint of a local minimum, which would imply an optimal toroidal rotation profile with respect to ion thermal confinement.

More complete analysis of momentum transport requires separating into the flux into a pinch, and even other terms like a residual stress [21]. This analysis is best done with perturbative type experiments and will be discussed in a future paper.

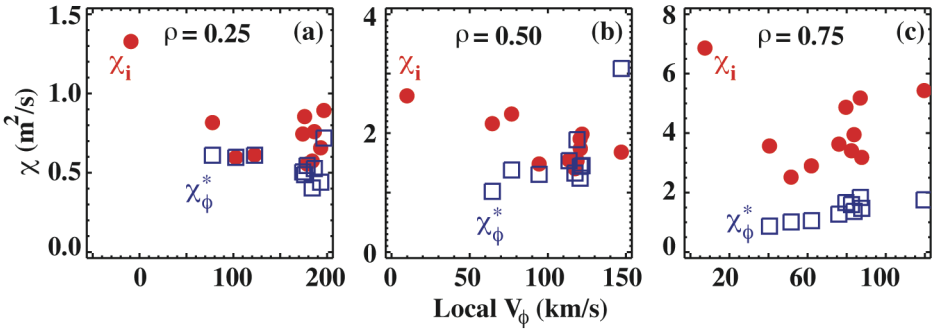
ρ = 0.25
(a)
ρ = 0.50
(b)
ρ = 0.75
(c)
χi
χφ*
χ (m²/s)
Local Vφ (km/s)
1.5
1.0
0.5
0.0
0
100
200
4
2
0
50
150
8
6
4
2
20
60

4. Effect of fast ion transport

The fast ion transport is of critical importance in being able to do momentum transport studies, since the torque deposited by the beams will obviously depend on where the fast ions are distributed. Frequently, when doing transport analysis with codes such as TRANSP, fundamental quantities such as the neutron rate appear to be overestimated by a significant fraction (typically 20-30%) compared with the measurements. Such discrepancies are commonly attributed to fast ion redistribution/losses associated with Alfvénic activity. These can be treated ad-hoc in TRANSP by means of an "anomalous beam ion diffusion" rate. The analysis presented so far does not consider any such anomalous beam ion diffusion.

In the ELMing H-mode plasmas described in section 2.1, a constant diffusion rate of up to $D_{\rm FI} \sim 2$ m^2/s was required to reduce the classically computed neutron rate down to the measured level. The associated reduction in fast ion pressure was also consistent with kinetic EFIT [26] reconstruction of the total pressure, accounting for the measured thermal pressure.

This level of anomalous beam ion diffusion can drastically change the total torque deposited to the plasma, although the effect on the torque is different for co and counter beams, and depends strongly on the anomalous diffusion profile, as well as the underlying model for the anomalous diffusion. For a constant anomalous diffusion across the plasma radius, co beams tend to lose co torque from the center, but also gain an additional *counter* $j \times B$ torque near the edge, associated with fast ions moving into regions of poor confinement (loss ion orbits). In these shots, the neutral beam torque can be reduced by up to 30% during the all co-beam phase. For counter beams, counter torque is reduced from the center, but approximately balanced by the increase in counter $j \times B$ torque at the edge. Hence, with such a model, the anomalous diffusion will make the total torque to the plasma more counter, although the degree to which this occurs is can be varied with different anomalous torque profiles.

Accordingly, the quantitative values of the momentum confinement times and angular momentum diffusivities presented in the preceding sections are subject to the details of the fast ion transport. However, the existence of a significant rotation at zero net applied torque and the anomalous torque profile cannot be explained by an anomalous fast ion diffusion. In particular, the need for an anomalous torque profile is actually amplified if there is significant fast ion redistribution. In the shot presented in figure 3, the neutral beam torque becomes even more negative than shown in figure 4 if $D_{\rm FI} > 0$ is used, indicating the need for an even greater anomalous torque, overplotted in figure 4. Interestingly, the torque density is reduced close to zero in the core and peaks up more at the edge, giving a profile that is more easily understood in terms of generation by strong edge gradients.

On the other hand, the response of the angular momentum to the applied torque becomes considerably more linear with the anomalous fast ion diffusion turned on. This is because the absolute reduction in the torque is greater at higher torque values where there are more co beams to be affected by the anomalous diffusion (so effectively the x-axis in figure 5 is compressed to the right). Hence, the degree of momentum confinement improvement at low torque is dependent on the details of the fast ion transport.

5. Summary

At moderate β_N levels in both H-mode plasmas with elevated $q_{\min}$ and hybrid plasmas, there is a significant intrinsic rotation in the co-direction at balanced neutral beam injection. The central rotation under such conditions can exceed 100 km/s. In fact, the rotation can remain positive even when the net neutral beam torque is negative everywhere across the profile. An anomalous torque profile was determined from the measurements, by determining how much additional (counter) neutral beam torque was required to reduce the plasma rotation to zero across the profile. In these plasmas, approximately one net counter neutral beam was required to achieve this, implying an anomalous source of torque in the plasma of about one neutral beam source. With such large intrinsic rotation profiles, it is important to factor in the intrinsic rotation in undertaking these momentum confinement studies.

Studies of global momentum confinement suggest that the confinement time depends on the applied neutral beam torque, even after consideration of the intrinsic rotation. Different dependences are observed in ELMing H-mode and hybrid plasmas, with the former showing a degradation in momentum confinement with increased torque, while the opposite effect is observed in the hybrids. It is speculated that the differing roles of $E \times B$ shear may be the source of this difference. Analysis of the local transport shows that the momentum and heat diffusivities respond quite differently to changes in torque/rotation in plasmas where $E \times B$ shear is not a strong effect. Finally, we have considered the potential complication of anomalous fast ion transport. If anything, including the effects of anomalous fast ion transport as indicated by the over-prediction of the neutron rate will only reinforce the results presented here, by requiring an even larger anomalous torque source. Nonetheless, fast ion transport is clearly an important area to pursue in the future in order to make progress in a fully quantitative understanding momentum transport in fusion plasmas.

References

[1] K. H. Burrell, Phys. Plasmas **4**, 1499 (1997).

[2] E. J. Strait, T. S. Taylor, A. D. Turnbull, J. R. Ferron, L. L. Lao, B. Rice, O. Sauter, S. J. Thompson, and D. Wróblewski, Phys. Rev. Lett. **74**, 2483 (1995).

[3] W. W. Heidbrink and G. J. Sadler, Nucl. Fusion **34**, 535 (1994).

[4] K.-L. Wong, Plasma Phys. Controlled Fusion **41**, R1 (1999).

[5] T. C. Hender, M. Gryaznevich, Y. Q. Liu, M. Bigi, R. J. Buttery, A. Bondeson, C. G. Gimblett, D. F. Howell, S. D. Pinches, M. de Baar, and P. de Vries, in Proceedings of the 20th IAEA Fusion Energy Conference, Villamoura, Portugal, 2004, http://www-naweb.iaea.org/napc/physics/fec/fec2004/datasets/EX_P2-22.html.

[6] R. J. La Haye, A. Bondeson, M. S. Chu, A. M. Garofalo, Y. Q. Liu, G. A. Navratil, M. Okabayashi, H. Reimerdes, and E.J. Strait, Nucl. Fusion **44**, 1197 (2004).

[7] L.-G. Eriksson, E. Righi, and K.-D Zastrow, Plasma Phys. Controlled Fusion **39**, 27 (1997).

[8] J. E. Rice, M. Greenwald, I. H. Hutchinson, E. S. Marmar, Y. Takase, S. M. Wolfe, and F. Bombarda, Nucl. Fusion **38**, 75 (1998).

[9] J. S. deGrassie, K. H. Burrell, L. R. Baylor, W. Houlberg, and J. Lohr, Phys. Plasmas **11**, 4323 (2004).

[10] J. S. deGrassie, J. E. Rice, K. H. Burrell, R. J. Groebner, and W. M. Solomon, Phys. Plasmas **14**, 056115 (2007).

[11] R. Isler, Phys. Rev. Lett. **38**, 1359 (1977).

[12] K. H. Burrell, D. H. Kaplan, P. Gohil, D. G. Nilson, R. J. Groebner, and D. M. Thomas, Rev. Sci. Instrum. **72**, 1028 (2001).

[13] K. H. Burrell, P. Gohil, R. J. Groebner, D. H. Kaplan, J. I. Robinson, and W. M. Solomon, Rev. Sci. Instrum. **75**, 3455 (2004).

[14] R. B. Howell, R. J. Fonck, R. J. Knize, and K. P. Jaehnig, Rev. Sci. Instrum. **59**, 1521 (1988).

[15] M. G. von Hellermann, W. Mandl, H. P. Summers, H. Weisen, A. Boileau, P. D. Morgan, H. Morsi, R. Koenig, M. F. Stamp, and R. Wolf, Rev. Sci. Instrum. **61**, 3479 (1990).

[16] W. M. Solomon, K. H. Burrell, P. Gohil, R. J. Groebner, and L. R. Baylor, Rev. Sci. Instrum. **75**, 3481 (2004).

[17] W. M. Solomon, K. H. Burrell, R. Andre, L. R. Baylor, R. Budny, P. Gohil, R. J. Groebner, C. T. Holcomb, W. A. Houlberg, and M. R. Wade, Phys. Plasmas **13**, 056116 (2006).

[18] R. J. Goldston, D. C. McCune, H. H. Towner, S. L. Davis, R. J. Hawryluk, and G. L. Schmidt, J. Comput. Phys. **43**, 61 (1981).

[19] N. Asakura, R. J. Fonck, K. P. Jaehnig, S. M. Kaye, B. LeBlanc and M. Okabayashi, Nucl. Fusion **33**, 1165 (1993).

[20] H. A. Claassen, H. Gerhauser, and A. Rogister, Phys. Plasmas **7**, 3699 (2000).

[21] O. D. Gurcan, P. H. Diamond, and T. S. Hahm, Phys. Plasmas **14**, 055902 (2007).

[22] J. E. Rice, P. T. Bonoli, J. A. Goetz, M. J. Greenwald, I. H. Hutchinson, E. S. Marmar, M. Porkolab, S. M. Wolfe, S. J. Wukitch, and C. S. Chang, Nucl. Fusion **39**, 1175 (1999).

[23] P.A. Politzer, C.C. Petty, R.J. Jayakumar, *et al*, in Proceedings of the 21st IAEA Fusion Energy Conference, Chengdu, China, 2006, http://www-naweb.iaea.org/napc/physics/fec/fec2006/papers/ex_p1-9.pdf

[24] R. E. Waltz, G.M. Staebler, W. Dorland, G.W. Hammett, M. Kotschenreuther, and J.A. Konings, Phys. Plasmas **4**, 2482 (1997).

[25] J.E. Kinsey, G.M. Staebler, R.E. Waltz, Phys. Plasmas **12**, 052503 (2005).

[26] L. Lao, H. St. John, R. Stambaugh, *et al.*, Nucl. Fusion **25**, 1611 (1985).

Acknowledgments

This work is supported by the U. S. Department of Energy under DE-AC02-76CH03073, and W-7405-ENG-48.